The effect of composition and holding time on glaze production using basalt rock as a base

David Candra Birawidha [1], Agus Miswanto[1], Liston Setiawan [1], Agus Prakosa [1], Umar Dani[1], Gunawan [1], Era Arianti [2], Pulung Karo-Karo [2], Totok Nugroho [3], Yusup Hendronursito [1,4]

[1] Research Center for Mining Technology - National Research and Innovation Agency (BRIN) Lampung – Indonesia

[2] Physics Department, Mathematics and Sciences Faculty (FMIPA) Universitas Lampung (Unila), Bandar Lampung – Indonesia

[3] Advanced Materials Research Center- National Research and Innovation Agency (BRIN), Kw. Puspiptek, Muncul, Kec. Setu, Kota Tangerang Selatan, Banten 15314, Indonesia

[4] Physics Department, Mathematics and Sciences Faculty (FMIPA) Universitas Gadjah Mada – Indonesia

Corresponding author: davi004@brin.go.id (David Candra Birawidha)

Abstract: This research studied the potential use of local basalt and feldspar from Lampung Province, Indonesia, as glaze materials. Frit(s) are composed of changing basalt-to-feldspar weight ratios of A (30:70), B (50:50), C (70:30), and D (100:0) w/w%. The added 20% boric acid to the total weight reduces the process temperature to 1,000^{o}C with holding times of 1, 4, and 8 hr(s). Based on the chemical composition test of the specimen, the four variations of the sample have SiO_2 content above 40%, and the average SiO_2/Al_2O_3 ratio is 4 and 5, which is usually a low-alumina glaze that will cause a glossy effect and have an amorphous structure. At point 2theta 29°, amorphous forms. Quartz (SiO_2), albite ($NaAlSi_3O_8$), anorthite ($CaAl_2Si_2O_8$), and coesite (SiO_2) phases were discovered in the glaze specimens. The anorthite phase in glass-ceramic glaze gives a transparent glaze color due to the amorphous glassy phase formed during heat treatment. The findings of this study suggest that local materials based on basalt and feldspar may be used as glaze materials to provide a smooth texture and surface; the glaze layer is evenly distributed, can follow the full surface contour of the test specimen, and has low porosity.

Keywords: basalt, feldspars, glaze, frits, crystal phase, sintering

1. Introduction

Ceramic is a material made from clay by going through the combustion process. The quality of clay ceramics is influenced by the raw materials used and the heating temperature (Rifai & Hartono, 2016). Glazed ceramics will add to its aesthetic value (Putra & Yana, 2020). Glaze in ceramics as a type of coating on certain types of ceramics to protect the surface and increase the aesthetic value of the product (Bormans, 2004). Glaze is a hygienic, decorative, glass-like coating that has chemical resistance (Prstić et al., 2007). To get the glaze with the desired combustion temperature, the selection of materials with the appropriate composition of ingredients is very important. The factors that influence the goodness or badness of a ceramic glaze layer are (a) glaze composition, (b) glazing method, (c) sintering time, (d) combustion temperature and (e) dissolved salts in clay (Arifin & Primadona, 2014). The glaze constituent materials broadly consist of glass formers as the frame structure of the glass phase, fluxes as materials for the formation of fused glass during the combustion process, and glass phase stabilizers as binders or stabilizers. adhesive to all existing materials.

Glazes with basalt as the main component can be used to protect, cover and decorate products made of different ceramic bodies (Andrić et al., 2012; Bayrak & Yilmaz, 2014; Gultekin E. E, 2018; Levitskii et al., 2013; Marica, 2004). Basalt itself has high mechanical capabilities, with good values of hardness and toughness, making it resistant to abrasion when applied as a glaze layer (Prstić et al., 2007). Additionally, basalt is readily available due to its widespread presence on the Earth's surface. According to geological studies (de Lima et al., 2022), 90% of surface volcanic rocks in the world are basalt, ensuring

its sustainability as a source of raw materials for glazes. However, one drawback of basalt as a glaze component is the difficulty in controlling the desired color because basalt contains a variety of mineral compositions, and each mineral plays a unique role in influencing the resulting color. The use of glaze as a coating is commonly used in decorative ceramics, ceramic tableware, and floor tiles. The use of glaze layers in addition to increasing aesthetic value, can also cover the surface porosity of the material, improve mechanical properties, increase friction resistance to chemical resistance (Casasola et al., 2012; Da Silva et al., 2012; Kalirajan et al., 2016; Sánches, 1997; Zhang et al., 2017). Glaze properties are usually influenced by chemical composition and combustion parameters, to physical properties, including color, glossy, and roughness of the final product (Ergin et al., 2023).

Basalt rock reserves in Indonesia reach more than one billion tons. Its presence in various regions in Indonesia ranging from Sumatra, Java, Kalimantan, Sulawesi and Papua (Isnugroho et al., 2020). Lampung Province volcanic products are scattered around the west side of Mount Tanggamus, through the bay around Semangko and continuing eastward to Mount Rajabasa and the basalt plateau in the Sukadana area. One of them is in East Lampung Regency with a basin-shaped characteristic (Muttaqii et al., 2020). Basalt stone from East Lampung is characterized by having holes around the stone, blackish brown on the outside and blackish ash on the inside (Hendronursito et al., 2018). One of the advantages of basalt rock is that the mechanical properties of the processed products can be modified as needed through the heat treatment method (Birawidha et al., 2021). In the case of basalt, processing it by applying slow cooling can provide mechanical properties that are more resilient in accepting impact loads, conversely by giving faster cooling, surface hardness can increase but has a high degree of brittleness. The same is the case for products made of metal, the process of increasing or modifying the mechanical properties of metals can be done by playing the temperature of the heat treatment or cooling. The temperature in the heat treatment process will determine the level of resistance and strength of the material. Therefore, it is necessary to conduct a research by engineering the heat treatment (Kurniawan & Setiyorini, 2014). The holding time is carried out to obtain the maximum hardness of a material in the heat treatment process by holding it at the hardening temperature to obtain homogeneous heating so that carbon diffusion occurs with alloying elements (Fadare et al., 2023). Basalt rock has a sufficient melting temperature (1,200°C), a flux in the form of boric acid is needed to lower the melting temperature. However, with a short holding time it is possible for the formation of an uneven (homogeneous) layer to occur. The research was conducted on the effect of composition and holding time on the melting temperature of basalt-based glaze products. The glaze is made with a composition of feldspar, bentonite, boric acid and basalt rock (Amin et al., 2019). The results of this research are expected to obtain the optimal composition for creating a glaze layer that can adhere well and cover the ceramic body's surface without defects, displaying a glossy and flat morphology. It is anticipated that by applying this basalt-based glaze at a maximum temperature of 1,000°C, it can be used for terracotta-type ceramic bodies made of clay, where the maximum firing temperature is 1,000°C.

2. Materials and methods

The production of glaze begins with preparing basalt, feldspar, boric acid and bentonite. Basalt, Feldspar, and bentonite are obtained from local mining in Lampung Province - Indonesia. Boric acid used from Sigma-Aldrich, CAS No. 10043-35-3.

The raw material is then sieved using a 100mesh sieve. Then mixing according to the calculation of variations in the mass ratio (wt%) of basalt vs feldspar: A (30:70); B (50:50); C (70:30); and D (100:0). The composition of the basalt and feldspar powders is then added with 20% boric acid of the total weight. The frit material is then stirred until homogeneous. Furthermore, combustion is carried out at a temperature of 1,000°C for 1 hour with a fast-cooling technique using water.

The frit is then ground and sieved using a 270 mesh sieves. The frit that has been smooth is added to 5% bentonite from weight total, then the glaze solution is made until it is homogeneous by adding water to each variation of the sample. Then dip the test medium in the form of refractory bricks into the glaze solution for 5 seconds and then drying the sample at room temperature. Then burn the glaze sample at a temperature of 1,000°C with variations in holding time of 1, 4 and 8 hours and cooling in the furnace.

The glaze will be characterized by using PanAnalytical Xpert 3 Powder X-RD with a Cu-Kα as a source of X-ray operating at 40 kV and 30 mA to obtain the crystallinity and phase data. The sample was scanned in the range 2θ of 0-80. The chemical compositions of basalt stone were characterized by Epsilon 4 XRF Spectrometer from Malvern PanAnalytical operating at 50 kV and 3 mA and FE-SEM Thermo Scientific Quattro S to observe the surface morphology and cross-section of the glaze. To determine the value of the density and porosity of the glaze using the ASTM C 373-88 standard in Eq. 1 and Eq. 2 (ASTM C373-88, 2006).

$$\rho = \frac{m}{v} \tag{1}$$

where ρ is density (g/cm³), m is mass of sample (g), and V is sample volume (cm³).

$$\% \ porosity = \frac{m_b - m_k}{\rho_{water} \ x \ V_t} x100\% \tag{2}$$

where mb is wet mass of sample (g), mk is dry mass of sample (g), ρ_{water} is density of water (g/cm³), and V_t is total sample volume (cm³).

3.   Results and discussion

3.1. Thermal analysis of glass fritz

DSC and Thermogravimetric analysis (TGA) comparison curve for glaze shown in Fig. 1. From the DSC glaze test, it appears that the glass transition temperature (Tg) occurs at a temperature of around 100°C. Precisely for speciments A, B, C, and D, they are 71°C, 92.3°C, 122°C, and 88.1°C, respectively. At this temperature, there was a mass decrease of 1.88%, 6.57%, 0.68%, and 0.22% for speciments A, B, C, and D. The sharp change in the curve for speciments C and D indicates a chemical reaction that caused an increase in bond density, cross-linking of materials, and reduced molecular mobility. The glass transition temperature (Tg), which increases sharply, is directly proportional to the increase in the degree of hardening. The area after the transition glass point (Tg) is related to the residual heat of reaction (ΔHR). The thermal heat capacities of speciments C and D are 287.6 J/g and 25.92 J/g, respectively. The area of the exothermic curves shows the highest thermal heat capacity in speciment B. speciments A and C have a thermal heat capacity of 1,188 J/g and 1,129 J/g, while sample B is 6,106 J/g, and the lowest is speciment D at 234.8 J/g. At this temperature, there was a significant decrease in mass in speciment C by 34.73% and in speciment A by 9.3%. Speciments B and D did not experience significant changes in mass.
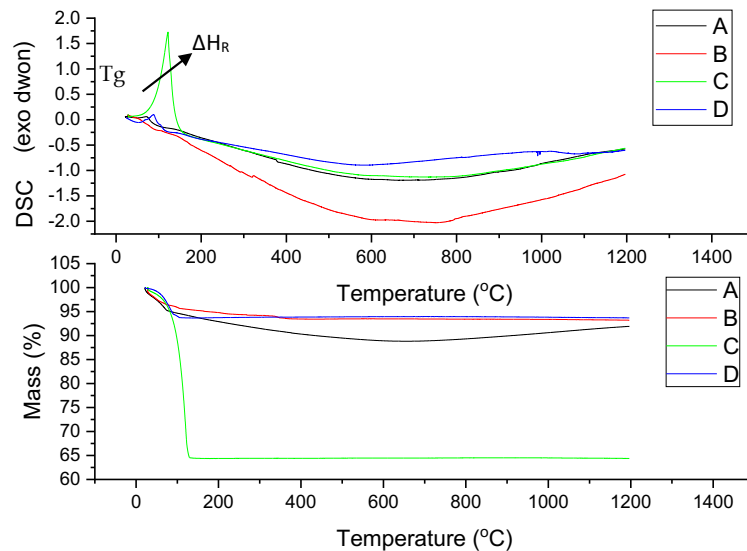
Fig. 1. DSC and Thermogravimetric (TGA) curve for glaze

3.2. Chemical composition

The result of chemical composition of raw materials shown in Table 1. Meanwhile, Table 2 shows the chemical composition of each sample.

Table 1. The results of the characterization of glaze raw materials using XRF

Compound	Basalt	Feldspar	Bentonite
SiO_2 (wt%)	44.83	55.86	62.12
Fe_2O_3 (wt%)	19.46	7.97	5.30
Al_2O_3 (wt%)	15.96	23.89	15.73
CaO (wt%)	13.01	-	3.68
MgO (wt%)	2.48	-	3.30
Na_2O (wt%)	3.35	-	-
TiO_2 (wt%)	1.86	1.12	-
P_2O_5 (wt%)	0.71	0.86	0.12
K_2O (wt%)	0.69	9.54	0.55
MnO (wt%)	0.45	0.23	0.07
Eu_2O_3 (wt%)	0.12	-	-
ZrO_2 (wt%)	-	0.39	-
NiO (wt%)	-	-	0.09
SO_3 (wt%)	-	-	0.15

Based on the results of XRF characterization in Table 1, it shows that the chemical composition of basalt is dominated by SiO_2, Fe_2O_3, Al_2O_3 and CaO compounds as well as other compounds, namely MgO, Na_2O, TiO_2, P_2O_5, K_2O, MnO and Eu_2O_3.

For feldspar raw material is in accordance with the feldspar content obtained in previous studies (Amin et al., 2019). The local feldspars in Lampung region have a chemical composition that is not too much different. The dominant chemical composition of feldspar includes silica (SiO_2), alumina (Al_2O_3), kalium oxide (K_2O) and iron oxide (Fe_2O_3). For bentonite, the chemical compounds that dominate are SiO_2, Al_2O_3 and Fe_2O_3 and other compounds are MgO, CaO, P_2O_5, K_2O, MnO, NiO and SO_3. This is in accordance with previous studies which stated that bentonite has a dominant chemical composition of SiO_2 (Drobíková et al., 2019).

Based on the results of XRF characterization in Table 2, it shows that the higher the percentage of basalt used, the compounds SiO_2, Al_2O_3, K_2O, P_2O_5 and ZrO_2 decreased while the compounds Fe_2O_3, CaO, Na_2O, TiO_2, MgO, MnO, Cr_2O_3, SrO and Eu_2O_3 increased.

Table 2. Result of frit glaze characterization using XRF

Compound	A	B	C	D
SiO_2 (wt%)	57.64	53.32	48.51	40.19
Al_2O_3 (wt%)	14.60	13.80	12.66	12.12
Fe_2O_3 (wt%)	10.16	13.62	17.76	22.66
K_2O (wt%)	7.116	4.94	3.18	0.93
CaO (wt%)	6.90	9.54	12.16	16.98
TiO_2 (wt%)	1.14	1.37	1.64	2.03
Na_2O (wt%)	1.27	1.8	1.98	2.3
MgO (wt%)	0.96	1.83	2.43	3.30
P_2O_5 (wt%)	0.81	0.76	0.77	0.74
MnO (wt%)	0.17	0.24	0.30	0.44
ZrO_2 (wt%)	0.12	0.10	-	-
Cr_2O_3 (wt%)	-	-	-	0.12
SrO (wt%)	-	-	-	0.10
Eu_2O_3 (wt%)	-	-	-	0.10

Main chemical composition of A, B, C, and D specimen consist of 40.19 – 57.64% SiO_2, 10.16 – 22.66% Fe_2O_3, 12.12 – 14.60% Al_2O_3, 6,9 – 16.98% CaO, 0.93 – 7.116% K_2O, 0.96 – 3.30% MgO, 1.14 – 2.03% TiO_2, respectively. While the minor chemical contents consist of P_2O_5, MnO, ZrO_2, Cr_2O_3, SrO, Eu_2O_3 less than 2wt%. The glass raw material in the form of glass will later be diluted with water to obtain a suspension of glass solution for application to the surface of the ceramic body specimen. Based on experience from purchases in the glazing sector, the proportion of silica needed to form a glass layer is at least above 30% (Suparta, 2008). In the frits material for this glaze, the four variations of the sample have SiO_2 content above 40%, and the average SiO_2/Al_2O_3 ratio is 4 and 5, which is usually a low alumina glaze which will cause a glossy effect and have an amorphous structure (Partyka et al., 2015).

Basalt rocks usually have a composition of SiO_2 ranging from 42 – 54%. Based on the relatively high SiO_2 compound, basalt is classified as tholeiitic (Philpotts & Ague, 2009). The iron-rich silicate composition found in basaltic rocks allows for changes in standard and natural raw materials, having good mechanical properties and thermal and chemical advantages (de Lima et al., 2021). Basalt melting or sinter-crystallization is very suitable for use as a coating material because of its long-term chemical stability. Iron oxide is present dominantly in basalt compared to the other two materials. This iron oxide's chemical composition will affect the resulting color (Sukmana et al., 2022).

Chemically feldspar is divided into potassium feldspar (chemical formula: $KAlSi_3O_8$), sodium feldspar (Chemical Formula: $NaAlSi_3O_8$), calcium feldspar (Chemical formula: $CaAl_2Si_2O_8$), and barium feldspar (Chemical Formula: $BaAl_2Si_2O_8$). If seen from the results of chemical composition testing, this feldspar from South Lampung does not have the elements CaO, NaO, and BaO. However, it has a dominant SiO_2, Al_2O_3, and K_2O content.

The dominant silicate content in basalt and alumina in feldspar gives the resulting glaze properties advantages. The combination of silicate-rich basalt with feldspar and bentonite, which is rich in alumina composition, produces a high refractory material with a low coefficient of thermal expansion (Abdel-Hameed & Bakr, 2007).

The more basalt used in glaze manufacture, the SiO_2 compounds as silica and Al_2O_3 as alumina decreased, while the compounds that acted as flux, namely Fe_2O_3, CaO, MgO, MnO, increased. Silica is the main ingredient for every type of glaze, where silica will form a layer of glass when it melts and will freeze after going through the cooling process. Alumina is binding as a hardening element and helps form a stronger layer of glaze. The increase in flux in the manufacture of glaze has a significant function in the melting of raw materials, changing the glass framework and as a decrease in melting temperature and provides a stabilizing effect on the glaze. In a previous study (Amin et al., 2019), the content of SiO_2 was 37.76 - 59.64%, Fe_2O_3 was 10.1 - 20.93%, and Al_2O_3 was 11.77 - 14.2%. For feldspar, the chemical composition is dominated by SiO_2, Al_2O_3, K_2O, and Fe_2O_3, as well as other compounds, namely TiO_2, P_2O_5, K_2O, MnO, and ZrO_2. The difference in raw basalt composition greatly affects the properties of glass ceramics (El-Shennawi et al., 1999). Specimens A and B have met the criteria for the SiO_2 component in crystalline frit material. The main component of SiO_2 is between 50 to 60wt% allowing crystalline frit to form, characterized by glossy, transparent, viscous, and low fusible properties (Amorós et al., 2013).

3.3. Crystalline phase

Fig. 2 compares the phase identification of crystalline material in specimen A, with holding times of 1, 4, and 8 hrs, while Fig. 3 is for specimen B, Fig. 4 is for specimen C, and Fig. 5 is for specimen D.

In glaze A, the highest intensity was at 2θ of 27.8049°, 27.297°, and 27.8522° for a holding time of 1, 4, and 8 hrs, respectively. The phase formed was the albite phase based on COD 96-900-1633 data with a chemical compound, namely Na ($AlSi_3O_8$), the anorthite phase based on COD 00-002-0523 data with a chemical compound, namely $CaAl_2Si_2O_8$ and a quartz phase with a chemical compound, namely SiO_2. Typically, albite and anorthite are always associated, forming a solid solution to become plagioclase (Reitze et al., 2021). Plagioclase itself can be found in basalt rocks, generally forming the crystal structure of the rock. Thus, when used as a glaze material, albite and anorthite still appear during the cooling process. Additionally, quartz is also observed to form alongside the development of plagioclase during the cooling process, due to the glaze sample itself being rich in SiO_2 compounds based on Table 2. The difference among the three glaze variations when held at 1,000°C is that the longer they are held, the

less quartz phase forms, with a tendency for albite or anorthite to increase with the additional time provided for crystal formation. For example, it is possible that sample A4 has undergone a phase transformation involving quartz at a specific temperature, allowing quartz to appear at the peak positions of 2θ around 40° and 70°. The appropriate holding time at that temperature may have provided an opportunity for this phase transformation to occur sufficiently, resulting in the detection of quartz peaks in the XRD pattern of sample A4.

On the other hand, samples A1 and A8 may not have undergone a phase transformation involving quartz at the same temperature, or perhaps they did not receive sufficient holding time for this transformation to occur completely. Therefore, even though they share the same peak positions at 2θ, samples A1 and A8 may not exhibit quartz peaks at those angles in the XRD pattern.

In other words, differences in phase transformation and holding time at a specific temperature can explain why sample A4 shows quartz peaks at 2θ 40° and 70°, while samples A1 and A8 do not exhibit similar peaks at those angles in the XRD pattern.

In glass B with a holding period of 1 hour, the highest intensity was at 2θ of 44.6996˚, the holding time was 4 hours, the highest intensity was at 2θ of 27.7852˚, the holding period was 8 hours, the highest intensity was at 2θ of 44.7072˚. The phase formed is the albite phase based on COD 96-900-1633 data with a chemical compound, namely Na $(AlSi_3O_8)$, anorthite phase based on COD 00-002-0523 data with a chemical compound, namely $CaAl_2Si_2O_8$ and the quartz phase based on COD 01-083-0541 data with a chemical compound, namely SiO_2. While in glaze C with a holding period of 1 hour, the highest intensity is at 2θ of 44.7036˚, the phase formed is the albite phase based on COD data 96-900-1633 with the chemical compound Na $(AlSi_3O_8)$, anorthite phase based on data COD 00-002-0523 with a chemical compound, namely $CaAl_2Si_2O_8$, Coesite phase based on COD data 01-072-1601 with chemical
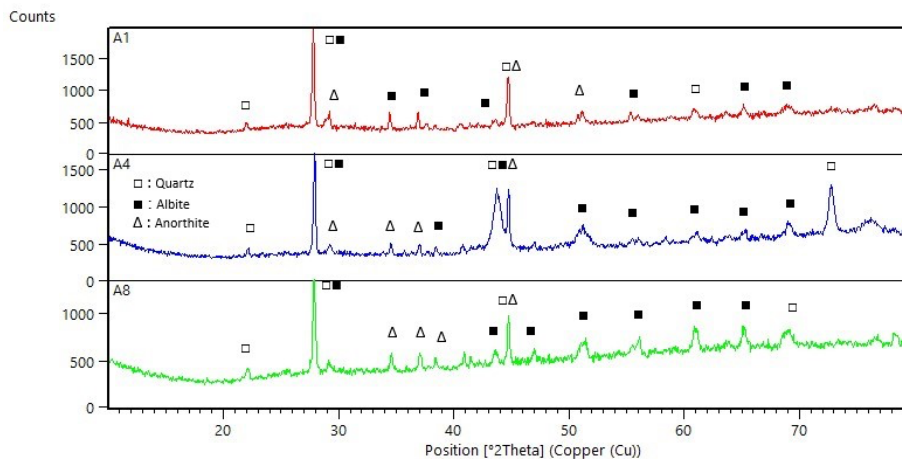
Fig. 2. X-ray diffraction (XRD) for specimen A
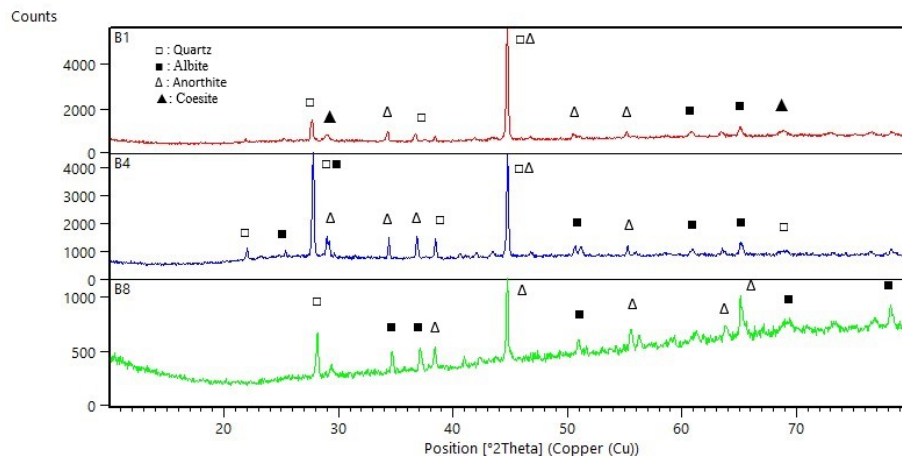
Fig. 3. X-ray diffraction (XRD) for specimen B
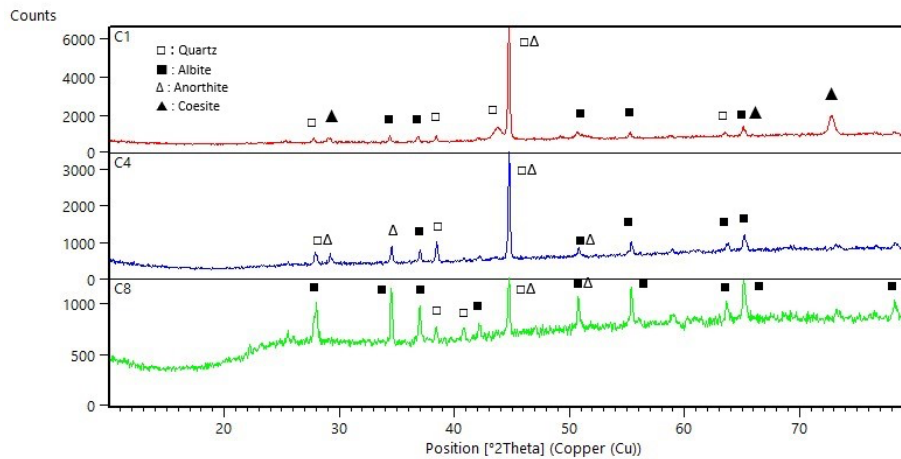
Fig. 4. X-ray diffraction (XRD) for specimen C

compound namely SiO_2 and quartz phase based on COD data 01-083-0541 with chemical compound SiO_2. There is an interesting phenomenon that occurs in samples B and C, specifically during the 1-hour holding period, coesite phase formation takes place during the crystallization of the glaze sample when the cooling process occurs. Based on various literature on coesite, this phase is one of the polymorphs of low quartz or alpha quartz under stable conditions. The formation of coesite theoretically should occur when quartz is subjected to high pressure and temperatures around 500 - 600°C or higher (Angel et al., 2001; Koike et al., 2013; Martell, 2016; Sasaki et al., 1983b). However, in the glaze-making process, quartz is only exposed to high temperatures at 1,000°C in an ambient pressure environment.

In a study by Martinez et al (2008), some coesite can form at a temperature of 565°C and low pressure, where amorf silica xerogel, serving as a source of quartz, is mixed with chlorophyll aggregates dispersed in amorphous silica (Martínez et al., 2008). Additionally, research by Sasaki et al (1983) showed that the synthesis of coesite from quartz, in the form of silica gel which is in amorf form, is facilitated by the addition of acid under high-pressure conditions (Sasaki et al., 1983a).

While in the glaze formation process, the sample is first turned into frit, to which borax flux is added, and then it is initially fired at 1000°C and rapidly cooled, resulting in the formation of an amorphous phase. Subsequently, during the second firing at 1,000°C after applying the glaze material to the ceramic body surface, the influence of the acid likely causes some of the quartz, which should have formed in an amorphous state, to transform into coesite, as shown in Figs. 2 and 3. Then, because coesite is an unstable polymorph of quartz, as the holding time during the cooling process increases, coesite transforms back into quartz or becomes undetectable due to being suppressed by the growth of the plagioclase solid solution, as seen in the other glaze samples (speciments A and D). Furthermore, based on Fig. 3, with the prolonged holding time under melting conditions, plagioclase (albite-anorthite) will grow dominantly, replacing quartz, where the silica in quartz is more prone to associate and form anorthite in sample B8, as in the study by Shi and partner in 2023, ceramics of anorthite were synthesized from quartz, mullite, and other materials derived from fly ash at high temperatures (Shi and Wang, 2023).

In Fig. 2, the intensity of sample A appears lower than the others. This could happen due to several reasons like even if the samples have the same phase, the crystal size and perfection can differ. Larger, more perfect crystals tend to produce stronger diffraction peaks. If one sample has larger or more well-formed crystals than the other, it can result in a higher peak intensity. Furthermore, the orientation of crystals within a sample can affect the intensity of diffraction peaks. If one sample has a preferred crystal orientation that enhances the diffraction of X-rays at a particular angle (such as the angle corresponding to theta 45°), it can lead to a higher peak intensity compared to a sample with a random or different crystal orientation. Additionally, the method used for sample preparation can influence the intensity of XRD peaks. Factors such as grinding, polishing, and particle size distribution can affect the crystal size and morphology, which in turn can impact the peak intensity.
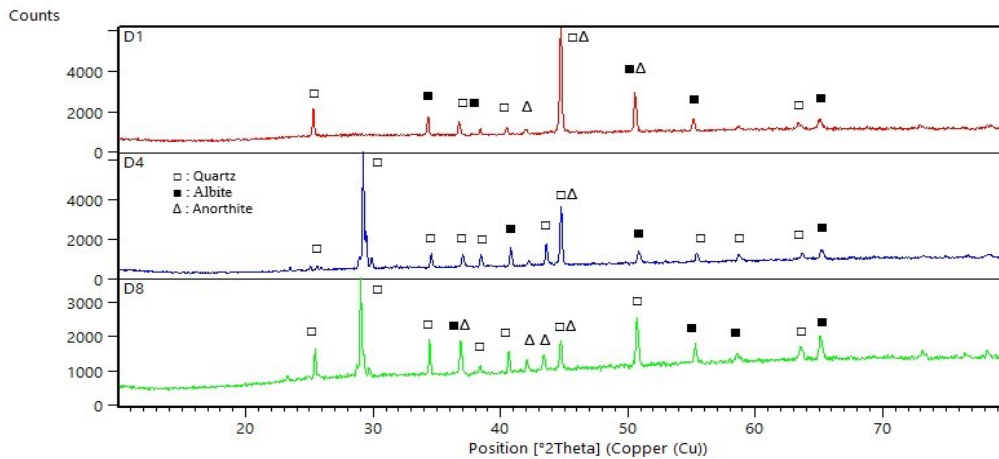
Fig. 5. X-ray diffraction (xrd) for specimen D

intensity was at 2θ of 29.0121˚. The phase formed is the albite phase based on COD 96-900-1633 data with a chemical compound, Na ($AlSi_3O_8$), anorthite phase based on COD 00-002-0523 data with a chemical compound, $CaAl_2Si_2O_8$, and a quartz phase based on data COD 01-083-0541 with a chemical compound, namely SiO_2.

As explained above, plagioclase is a combined phase between albite ($NaAlSi_3O_8$) and anorthite ($CaAl_2Si_2O_8$), where the two will constantly interact as a solid solution. The two will always be associated, especially in glazes based on Lampung basalt rocks containing relatively high plagioclase (Muttaqii et al., 2020). From the XRD data in Fig. 2-5 above, by extending the holding time during the glaze-making process, sometimes albite will replace anorthite and vice versa, only with a difference in the amount of intensity in each holding time. Plagioclase feldspar is a series of continuous minerals where calcium and sodium will replace one another in the same crystal structure (Mookherjee et al., 2016). The role influence of the composition of the glaze forming can also trigger a tendency to dominate the formation of legible albite and anorthite. In speciments A, B, and C, by extending the holding time for making the glaze, several SiO_2 compounds read from quartz and coesite tended to associate to form feldspar plagioclase bonds. This phenomenon is influenced by the reduced feldspar composition triggering SiO_2 to associate more to form aluminosilicate (Min et al., 2019).

The phases formed in the characterization of B8 and C1 glaze have similarities with the phases formed in the study (Andrić et al., 2012) including olivine, anorthite, and pyroxene phases. In another study, it was also stated that the phases formed were magnetite, anorthite and quartz (Gultekin E. E, 2018). The dominant anorthite phase gives an advantage overglaze. Anorthite ($CaAl_2Si_2O_8$) on glass ceramic bodies has a low dielectric constant, dc volume resistivity, and low ac dielectric discharge (Abdel-Hameed & Bakr, 2007). The anorthite phase in glass-ceramics glaze gives a transparent glaze color due to the amorphous glassy phase formed during heat treatment. The anorthite phase in the crystalline frit is a concern for developing transparent glass ceramics with high hardness for ceramic tiles. In previous studies, it was explained that adding boron can increase the size of anorthite, thereby reducing light scattering and increasing transparency (Wang S et al., 2022).

The quartz phase in the specimens was assumed to be from insensitive raw materials and was mainly observed on glass quickly. Calcium oxide found in basalt and bentonite supports the formation of albite-type crystals. As explained in previous studies that the dissolution of lime in feldspar-rich melts supports the formation of albite-type crystals (Fröberg et al., 2007).

The crystallinity index in XRD data patterns can be calculated using the method of comparing the ratio of the total area under crystalline peaks to the total area under crystalline peaks plus the amorphous phase. The amorphous phase peaks appear as noise in the XRD data, while the crystalline peaks plus amorphous are represented by the overall XRD data obtained. Based on Table 3, in general, an increased usage of basalt results in a greater amount of crystallinity formed. The holding time during the glaze-making process itself does not significantly impact the quantity of crystalline formation. The holding time only affects the homogeneity of the glaze material melting process to ensure complete

melting. Sometimes, by allowing more time for the liquid homogenization process, due to the influence of higher levels of a particular element, there is a tendency for the formation of new phases to occur, displacing the previous phase-forming elements because the reactivity of the new element surpasses the one that was previously dominant.

From the perspective of elemental composition analysis and phase changes occurring during the firing process with different holding times, based on Table 3, the addition of basalt leads to an overall increase in crystallization in the glaze layer. Furthermore, according to Table 2, with the addition of basalt, CaO and Na_2O levels increase, stimulating the growth of plagioclase (albite-anorthite) during a longer homogenization process linearly correlated with extended holding times, as observed in Figs. 2-5. During the cooling process, quartz itself tends to bond with calcium or sodium, forming anorthite or albite.

Table 3. Quantitative data of crystalline and amorphous phase in glaze sample.

Glaze Sampel	Crystalline Phase (%)	Amorphous Phase (%)
A1	67,4	32,6
A4	65,7	34,3
A8	75,5	24,5
B1	76,4	23,6
B4	79,3	20,7
B8	75,8	24,2
C1	74,4	25,6
C4	84,6	15,4
C8	77,4	22,6
D1	88,3	11,7
D4	87,6	12,4
D8	89,8	10,2

3.4. Density & porosity

The results of the density test of the glaze and fire brick samples (as a control) using the ASTM C 373-88 standard are shown in Fig. 6.

	A	B	C	D	Refractory stone
1	2.192792502	2.151542575	2.321020156	2.384453782	2.091291062
4	2.533189887	2.39638009	2.356060606	2.330046791	2.091291062
8	2.410825578	2.288440971	2.356890169	2.372918979	2.091291062

Glaze Composition
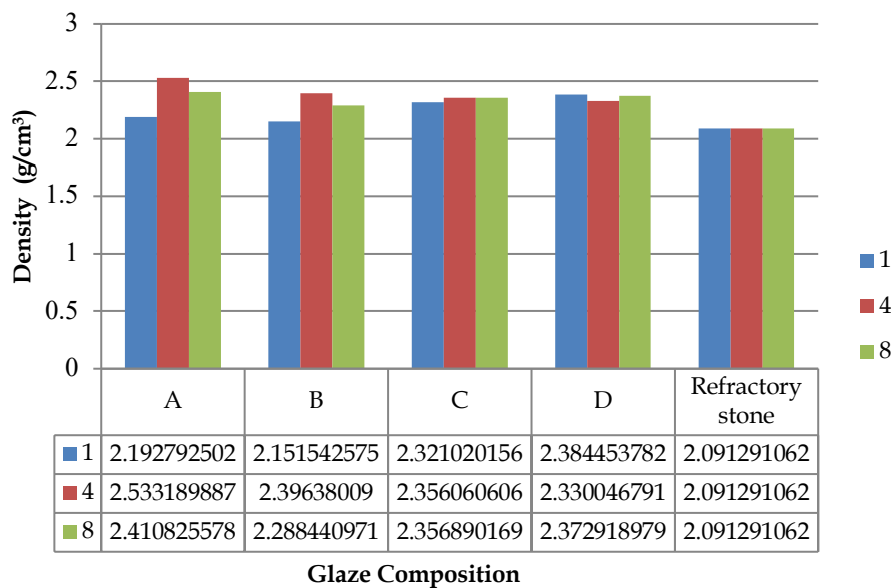
Fig. 6. Results of glaze and fire brick density tests

Fire brick as the biscuit has a density value of 2.09 g/cm³. The density values of samples A1, A4, and A8 were 2.19 g/cm³, 2.53 g/cm³, and 2.41 g/cm³ respectively. The density values of samples B1, B4, and B8 were 2.15 g/cm³, 2.39 g/cm³, and 2.28 g/cm³ respectively. The density values of samples C1, C4, and C8 were 2.32 g/cm³, 2.35 g/cm³, and 2.35 g/cm³ respectively.

The maximum density value occurs in glaze sample A4, 2.53 g/cm³, and the minimum in glaze sample B1, 2.15 g/cm³. Based on Fig. 5, after the glazing process, the sample's density will increase by approximately 0.06 g/cm³ to 0.44 g/cm³. The highest density in the A4 specimen has the highest amorphous phase, namely 34.3%. When compared with the lowest density, specimen B1 has an armorphous phase of 23.6%. However, the dominant amorphous phase does not significantly influence the density. If we look at the crystal phase that is formed, specimen A4 has three dominant crystal phase points with the quartz, anorthite, and albite phases. Meanwhile, in specimen B1, the dominant crystal phase is formed at $2\theta = 44.7°$ with quartz and anorthite crystal phases. The dominance of the crystalline and amorphous phases influences the glaze density. On the other hand, the high density is directly proportional to the added thickness of the layer that can form. The thicker the layer, the higher the density will be. Since the glaze thickness cannot be controlled during the dipping process of the biscuit into the glaze solution, the thickness that occurs varies among glaze samples. The density glaze is higher than the fire brick. In several previous studies, the density of glaze products with basalt was between 1.45 – 1.5 g/cm³, a maximum of 2 g/cm³ (Andrić et al., 2012). This density difference is influenced by the percentage of basalt material made as a glaze.

Furthermore, the results of the porosity test of the glaze and fire brick samples (as a control) using the ASTM C 373-88 standard are shown in Fig. 7.

Glaze Composition	A	B	C	D	Refractory stone
1	20.7659987	21.0941999	21.0119292	17.6955398	21.7914439
4	19.3867671	21.4232826	21.506734	20.7553476	21.7914439
8	20.8998549	16.6351296	20.2056767	20.4729787	21.7914439
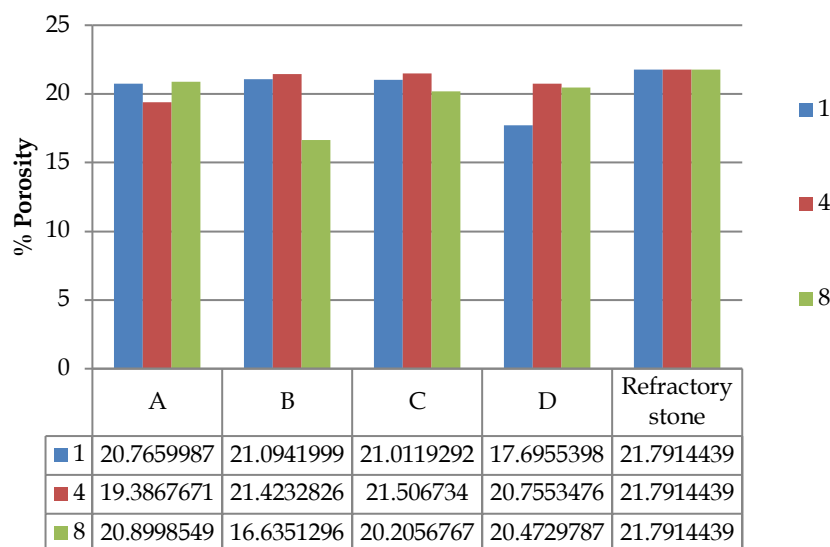
Fig. 7. Porosity test results for glaze and fire bricks

Based on the porosity test in Fig. 7, it shows that the fire brick as bisquit has a porosity value of 21.79%. The porosity values of samples A1, A4 and A8 were 20.76%, 19.38% and 20.89% respectively. The porosity values of samples B1, B4 and B8 were 21.09%, 21.42% and 16.63% respectively. The porosity values of samples C1, C4 and C8 were 21.01%, 21.5% and 20.2% respectively. The porosity values of samples D1, D4 and D8 were 17.69%, 20.75%, 20.47%, respectively. The maximum porosity value occurs in glaze sample C1 which is 21.01% and the minimum in glaze sample B8 is 16.63%. The maximum porosity value is caused by hairline cracks in the glaze C1 so that the surface of the glaze is not completely covered. Temperature and holding time differences affect the crystal structure, density, and porosity. The organic material from the bentonite mixture undergoes oxidation during the sintering process, contributing to the glaze's high and low porosity. Based on the x-ray diffraction results in Fig.

2 – 5, it can be seen that several specimens at position 2theta < 29º do not form crystalline or amorphous phases. A comparison of the glass composition to the crystal structure formed shows that there are differences in density and porosity that occur.

3.5. Macro and micro photos

The different chemical composition and holding time of each sample have a different color effect. The color differences between each sample can be seen, as shown in Fig. 8.

a)	L*a*b* color difference $\Delta L^* = -39.82$ $\Delta a^* = +13.48$ $\Delta b^* = +0.32$ $\Delta E^* = 42.04$	b)
L* = 74.93 a* = 4.95 b* = 2.58		L* = 35.11 a* = 18.43 b* = 2.90
c)	L*a*b* color difference $\Delta L^* = -29.2$ $\Delta a^* = -10.04$ $\Delta b^* = -1.28$ $\Delta E^* = 30.9$	d)
L* = 65 a* = 10.27 b* = 2.48		L* = 35.8 a* = 0.23 b* = 1.20
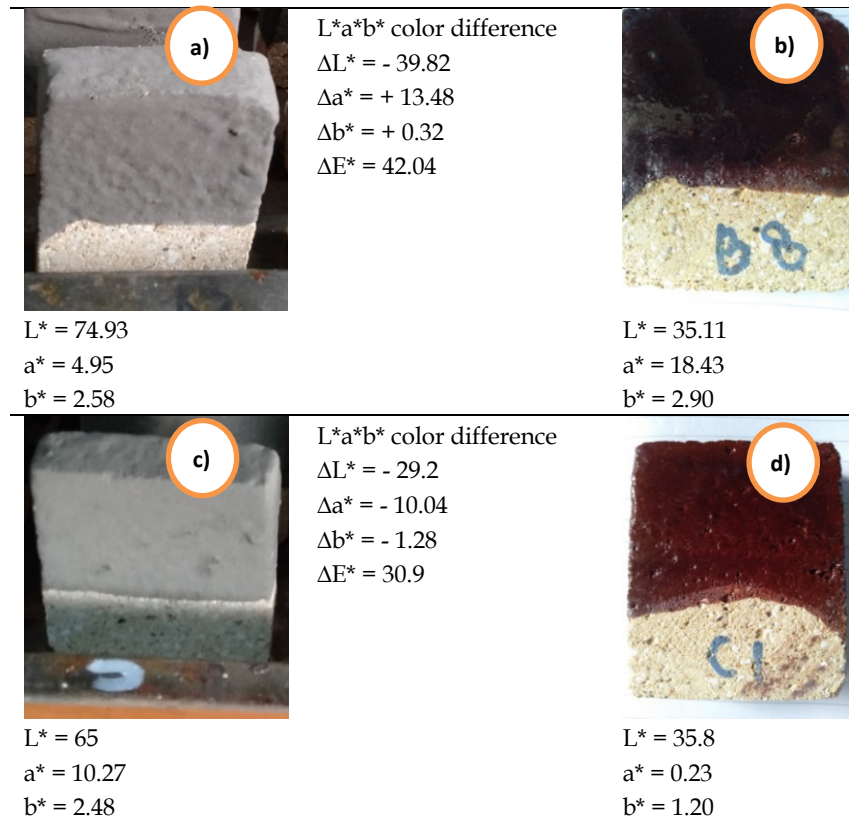
Fig. 8. Colorimeter test

The glaze sample before being fired was light gray in color, the texture was still a fine powder, and the layer was even on the entire test object. There is a striking color difference between the pretreatment and the glaze color, from gray to dark brown. Based on colorimeter testing, pretreated samples have higher brightness values than samples that have undergone combustion. The fritz in sample B8 is brighter, less red, and has almost the same yellowness compared to sample fritz C. The level of brightness in the short-burning sample is not much different from the long-burning sample, as indicated by the value $\Delta L^* = +0.69$. However, samples with a longer holding time were much more reddish in color than samples with a short heat treatment. The total color difference of the samples is $\Delta E^* = 18.3$.

Metal oxides in the chemical composition of the glaze influence the color change of the glaze material before firing, with time variations of 1, 4, and 8 hours. When seen in Table 2, iron oxide is dominant and increases from 10.16 wt% in sample A to 22.66 wt% in sample D, along with the addition of basalt. In accordance with previous research, melting basalt, which is rich in Fe oxide, will result in a brown color of glass ceramics (Sukmana et al., 2022). In this case, Fe_2O_3, TiO_2, and CuO compositions act as coloring agents. The distribution of transition metals such as Fe^{3+}/Fe^{2+}, Cr^{3+}, Ni^{2+}, Ti^{4+}, and Cu^+ causes variations in the selective absorption of visible light. The valence electrons of this ion jump between different energy levels to produce different colors (Shang et al., 2021).

We compared SEM photos for specimens B and C, where these two specimens had visible differences in micro. The characterization results SEM on the surface and cross-section of the B8 glaze shown in Fig. 9.
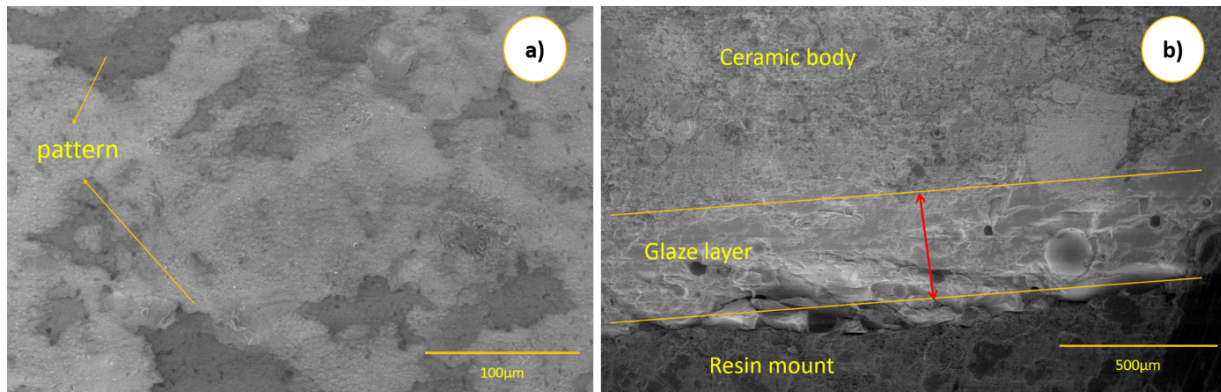
Fig. 9. The results of the characterization of B8 glaze using SEM; a) 1000x magnification on the surface; and
b) 200x on the cross section

Fig. 9 (a) shows that the characterization of SEM with 1000x magnification on the surface of the B8 glaze has a fine structure and coats all test specimens well because the surface is flat and there are no pores on the surface of the glaze. There are no defects or cracks on the surface of the glaze. From Fig. 9 (a), it can be observed that there are pattern variations in the form of dots at some points, which occur due to the influence of metal element precipitation within the glaze material composition (Birawidha et al., 2023). Fig. 9 (b) shows that the SEM characterization with a magnification of 200x on the cross section of B8 glaze has an average thickness ($\bar{l}$) of 383.62 μm and the glaze adheres perfectly to the test specimen well because the glaze is able to enter the pores of the test specimen.

The characterization results SEM on the surface and cross-section of the C1, glaze shown in Fig. 10. Fig. 10 (a) shows that the SEM characterization with 1000x magnification on the surface of the C1 glaze has a smooth structure and coats all test specimens well because the surface is flat and there are no pores on the glaze surface, but there are cracks at some area in the surface of the glaze. Furthermore, there are visible blisters or lumps at some points on the glaze surface, which may be attributed to the imperfect melting process of the glaze material with only a 1-hour holding time, causing excess elements to sometimes precipitate and form lumps on the glaze surface (Birawidha et al., 2023). Fig. 10 (b) shows that the SEM characterization with 200x magnification on the cross section of the C1 glaze has an average thickness ($\bar{l}$) is 172.41 μm and the glaze adheres perfectly to the test specimen well because the glaze is able to enter the pores of the test specimen. In the process of applying the glaze material to the surface of ceramic body or biscuit, it is done through a dipping process for 5 seconds. In theory, with the same immersion time, the glaze layer thickness should have the possibility of being the same (Baharav et al., 1999). However, in practice, the obtained thickness tends to vary within a certain range due to factors such as viscosity, surface adhesion-cohesion, and the preparation process. Therefore, in practical glazing work conducted by glaze practitioners, the spray technique is often used to control the thickness of the glaze obtained. In this study, because the glaze thickness was not controlled, the average glaze thickness obtained ranged from 150 microns to 400 microns.
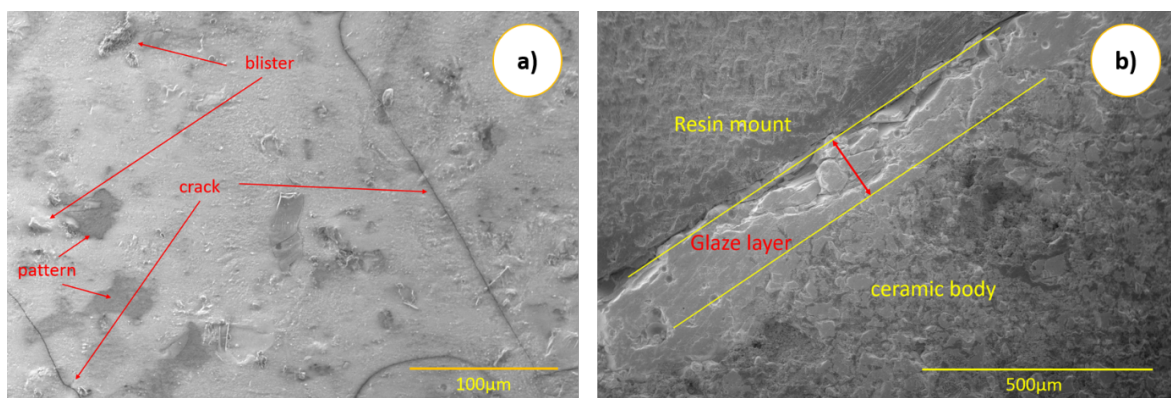
Fig. 10. The results of the characterization of C1 glaze using SEM; a) 1000x magnification on the surface; and
b) 200x on the cross section

4. Conclusions

Based on the research that has been done, it can be concluded that variations in the composition of the glaze material and holding time can affect the crystal structure and chemical content of the glaze.

1. The more basalt percentage used, the SiO_2, Al_2O_3 compounds decreased while the Fe_2O_3 compounds increased.
2. The phases that often appear are albite, anorthite and quartz. Meanwhile, the coesite phase only appears in samples B1 and C1.
3. The glaze that has the best results is glaze sample B8 because it has a smooth texture and surface, the glaze layer is evenly distributed and can follow the entire surface contour of the test specimen and has a low porosity value of 16.63%. While the glaze that had poor results was the C1 glaze sample because it had a rough texture and surface, there were hair cracks on the glaze surface, causing a high porosity value of 21.01%. Basalt as a material for glaze production has the potential to be explored further. Besides being readily available and cost-effective, the morphological and characteristic properties of its application as a glaze show promising results. However, additional research is needed to determine the optimal composition required. Furthermore, because basalt is rich in metallic minerals that can affect color, it is essential to add other elements to mitigate the influence of these metallic elements and achieve the desired color.

Acknowledgments

References

ABDEL-HAMEED, S. A., BAKR, I. M. 2007. *Effect of alumina on ceramic properties of cordierite glass–ceramic from basalt rock.* Journal of the European Ceramic Society, 27(2–3), 1893–1897.

AMIN, M., SUPRIYATNA, Y. I., HENDRONURSITO, Y., BIRAWIDHA, D. C., MAULIDA, LATIFAH, KAROKARO, P. 2019. *Addition of feldspart minerals as a substitution material on ceramics clay manufacture.* IOP Conference Series: Materials Science and Engineering, 478(1).

AMORÓS, J. L., GÓMEZ-TENA, M. P., MORENO, A., BLASCO, E., COOK, S., GALINDO, M. 2013. *Dissolution, crystallisation, and sintering of a raw matt glaze for porcelain tiles.* Advanced Materials Research, 704, 132–140.

ANDRIĆ, L., AĆIMOVIĆ-PAVLOVIĆ, Z., TRUMIĆ, M., PRSTIĆ, A., TANASKOVIĆ, Z. 2012. *Specific characteristics of coating glazes based on basalt.* Materials and Design, 39, 9–13.

ANGEL, R. J., MOSENFELDER, J. L., SHAW, C. S. J. 2001. *Anomalous compression and equation of state of coesite.* Physics of the Earth and Planetary Interiors, 124(1–2), 71–79.

ARIFIN, D. N., PRIMADONA, L. 2014. *Pengembangan Glasir Non-Timbal Berbahan Baku Limbah Tufa Andesit Untuk Memenuhi Syarat Mutu Glasir Genteng Keramik Berdasarkan Sni.* Prosiding Pemaparan Hasil Penelitian Pusat Penelitian Geoteknologi LIPI Tahun 2014, 978–979.

ASTM C373-88. 2006. ASTM C373-14 *Standard Test Method for Water Absorption, Bulk Density, Apparent Porosity, and Apparent Specific Gravity of Fired Whiteware Products.* Astm C373-88, 88(Reapproved), 1–2.

BAHARAV, H., LAUFER, B. ., PILO, R., CARDASH, H. S. 1999. *Effect of glaze thickness on the fracture toughness and hardness of alumina-reinforced porcelain.* The Journal of Prosthetic Dentistry, 81(5), 515–519.

BAYRAK, G., YILMAZ, S. 2014. *Granite based glass-Ceramic materials.* Acta Physica Polonica A, 125(2), 623–625.

BIRAWIDHA, D. C., ASMI, D., SEMBIRING, S., SUMARDI, S., BAHFIE, F., SUSANTI, D. 2023. *Characterization of the Glass Structure of East Lampung's Scoria Basalt (Indonesia) Applied to the Ceramic Body.* Powder Metallurgy and Metal Ceramics, 61(11–12), 699–707.

BIRAWIDHA, D. C., ISNUGROHO, K., HENDRONURSITO, Y., AMIN, M., MUTTAQII, M. AL, ALIMUDDIN, Z., RAJAGUKGUK, T. O. 2021. *Potential of basalt rock as a filler in polymer composite through the process of melting basalt combined with slow cooling.* Proceedings Of The 7th International Symposium On Applied Chemistry, Vol. 2493, No. 1.

BORMANS, P. 2004. *Ceramics are more than clay alone.* In Cambridge International Science Publishing.

CASASOLA, R., RINCÓN, J. M., ROMERO, M. 2012. *Glass-ceramic glazes for ceramic tiles: A review.* Journal of Materials Science, 47(2), 553–582.

DA SILVA, R. C., PIANARO, S. A., TEBCHERANI, S. M. 2012. *Preparation and characterization of glazes from combinations of different industrial wastes.* Ceramics International, 38(4), 2725–2731.

DE LIMA, L. F., PEROTTONI, C. A., ZORZI, J. E., CRUZ, R. C. D. 2021. *Effect of iron on the microstructure of basalt glass-ceramics obtained by the petrurgic method.* International Journal of Applied Ceramic Technology, 18(6), 1950–1959.

DE LIMA, L. F., ZORZI, J. E., CRUZ, R. C. 2022. *Basaltic glass-ceramic: A short review.* Boletín de La Sociedad Española de Cerámica Ya Vidrio, 61(1), 2–12.

DROBÍKOVÁ, K., ŠTRBOVÁ, K., TOKARCÍKOVÁ, M., MOTYKA, O., SEIDLEROVÁ, J. 2019. *Magnetically modified bentonite: Characterization and stability.* Materials Today: Proceedings, 37, 53–57.

EL-SHENNAWI, A. W. A., MANDOUR, M. A., MORSI, M. M., ABDEL-HAMEED, S. A. 1999. *Monopyroxenic basalt-based glass-ceramics.* Journal of the American Ceramic Society, 82(5), 1181–1186.

ERGIN, H., YILDIRIM, Y., ÇIRPIN, A., TURGUT, H., KAYACI, K. 2023. *Technological and economical investigation of glaze preparation using dry stirred media mill.* 59(5).

FADARE, D. A., FADARA, T., AKANBI, O. 2023. *Effect of Heat Treatment on Mechanical Properties and Microstructure of Advanced High-Strength Steel.* Metal Science and Heat Treatment, 64(9–10), 522–527.

FRÖBERG, L., KRONBERG, T., HUPA, L., HUPA, M. 2007. *Influence of firing parameters on phase composition of raw glazes.* Journal of the European Ceramic Society, 27(2–3), 1671–1675.

GULTEKIN E. E. 2018. *Transparent Glazes With Basalt Addition.* 19th International Metallurgy and Materials Congress, UCTA Chamber of Metallurgical and Materials Engineers Training Center, 433–436.

HENDRONURSITO, Y., BARUS, J., AMIN, M., MUTTAQII, M. AL, RAJAGUKGUK, T. O., ISNUGROHO, K., BIRAWIDHA, D. C. 2018. *The local mineral potential from East Lampung - Indonesia: the use of basalt rock as a stone meal for cassava plant Yusup.* J. Degraded Min. Lands Manag., 5(53), 2502–2458.

ISNUGROHO, K., BIRAWIDHA, D. C., HENDRONURSITO, Y., AMIN, M., MUTTAQII, M. AL, EFRIYO HADI, R. A., FAZMA, M. F. 2020. *Preliminary Study of Melting Basalt Rock As A Raw of Advanced Material.* IOP Conference Series: Materials Science and Engineering, 807(1).

KALIRAJAN, M., RANJEETH, R., VINOTHAN, R., VIDYAVATHY, S. M., SRINIVASAN, N. R. 2016. *Influence of glass wastes on the microstructural evolution and crystallization kinetics of glass-ceramic glaze.* Ceramics International, 42(16), 18724–18731.

KOIKE, C., NOGUCHI, R., CHIHARA, H., SUTO, H., OHTAKA, O., IMAI, Y., MATSUMOTO, T., TSUCHIYAMA, A. 2013. I*nfrared spectra of silica polymorphs and the conditions of their formation.* Astrophysical Journal, 778(1).

KURNIAWAN, B. E., SETIYORINI, Y. 2014. *Pengaruh variasi Holding Time Pada Perlakuan Panas Quench Annealing Terhadap Sifat mekanik dan Mikro Struktur Pada Baja mangan AISI 3401.* Jurnal Teknik POMITS, 3(1), 1–4.

LEVITSKII, I. A., POZNIAK, A. I., BARANCEVA, S. E. 2013. *Effects of the basaltic tuff additions on the properties, structure and phase composition of the ceramic tiles for interior wall facing.* Procedia Engineering, 57, 707–713.

MARICA, S. 2004. *Quaternary Basalts From Romania - Characteristics and Non-Conventional Uses.* Bulletin of the Geological Society of Greece, 36(1), 103.

MARTELL, J. 2016. *A study of shock - metamorphic features in zircon from the Siljan impact structure,* Sweden. 482(23), 15.

MARTÍNEZ, J. R., VÁZQUEZ-DURÁN, A., MARTÍNEZ-CASTAÑÓN, G., ORTEGA-ZARZOSA, G., PALOMARES-SÁNCHEZ, A., RUIZ, F. 2008. *Coesite Formation at Ambient Pressure and Low Temperatures.* Advances in Materials Science and Engineering, 2008 Artic, 1–6.

MIN, H., ZHANG, T., LI, Y., ZHAO, S., LI, J., LIN, D., WANG, J. 2019. *The albitization of k-feldspar in organic-and silt-rich fine-grained rocks of the lower cambrian qiongzhusi formation in the southwestern upper yangtze region, china.* Minerals, 9(10), 1–22.

MOOKHERJEE, M., MAINPRICE, D., MAHESHWARI, K., HEINONEN, O., PATEL, D., HARIHARAN, A. 2016. *Pressure induced elastic softening in framework aluminosilicate- albite (NaAlSi3 O8).* Scientific Reports, 6(9), 1–10.

MUTTAQII, M. AL, AMIN, M., HANDOKO, A. S., BIRAWIDHA, D. C., MUTTAQII, M. AL, AMIN, M., HANDOKO, A. S., BIRAWIDHA, D. C., ISNUGROHO, K., HENDRONURSITO, Y. 2020. *The characterization and physical properties of paving block products over basalt minerals.* 050006(April), 050006–1.

PARTYKA, J., SITARZ, M., LEŚNIAK, M., GASEK, K., JELEŃ, P. 2015. T*he effect of SiO$_2$/Al$_2$O$_3$ ratio on the structure and microstructure of the glazes from SiO2-Al 2O3-CaO-MgO-Na2O-K2O system.* Spectrochimica Acta - Part A: Molecular and Biomolecular Spectroscopy, 134, 621–630.

PHILPOTTS, A., AGUE, J. 2009. *Principles of Igneous and Metamorphic Petrology.* In Principles of Igneous and Metamorphic Petrology (2nd ed.). Cambridge University Press.

PRSTIĆ, A., AĆIMOVIĆ-PAVLOVIĆ, Z., PAVLOVIĆ, L., ANDRIĆ, L., TERZIĆ, A. 2007. T*he Application Of Basalt In The Manufacturing Of Ceramic Glazes.* Journal of Mining and Metallurgy, 43(A), 53–60.

PUTRA, N. S. D., YANA, D. 2020. P*emanfaatan Abu Kayu sebagai Bahan Aditif Glasir Suhu Tinggi.* Jurnal Sosioteknologi, 18(3), 543–559.

REITZE, M. P., WEBER, I., MORLOK, A., HIESINGER, H., BAUCH, K. E., STOJIC, A. N., HELBERT, J. 2021. *Mid-infrared spectroscopy of crystalline plagioclase feldspar samples with various Al,Si order and implications for remote*

sensing of Mercury and other terrestrial Solar System objects. Earth and Planetary Science Letters, 554, 116697.

RIFAI, M., HARTONO, S. B. 2016. *Pengaruh Proses Sintering Pada Temperatur 800ºC Terhadap Kekerasan dan Kekuatan Bending Pada Produk Gerabah*. Jurnal Traksi Universitas Muhammadiyah Semarang, 16(2), 1–9.

SÁNCHES, E. 1997. *Matérias-Primas para a Fabricação de Fritas e Esmaltes Cerâmicos Introdução Matérias-Primas para a Fabricação*. Cerâmica Industrial, 2(3/4), 32–40.

SASAKI, S., CHEN, H.-K., PREWITT, C. T., NAKAJIMA, Y. 1983a. *Re-examination of "P21/a" coesite*. Zeitschrift Für Kristallographie, 164, 67–77.

SASAKI, S., CHEN, H., PREWITT, C. T., NAKAJIMA, Y. 1983b. *Re-examination of " P 21 / a coesite "*. 77, 67–77.

SHI, Z., HAN, C., WANG, W. (2023). P*reparation and Properties of Quartz-Anorthite Ceramics Synthesized Using Desert Sand and Coal Fly Ash.* Journal of Materials in Civil Engineering, 35(8), 04023221.

SUKMANA, I., HENDRONURSITO, Y., SAVETLANA, S., ISNUGROHO, K., AMIN, M., BIRAWIDHA, D. C. 2022. *Characterization and Potential Production of Glass-Ceramics Biomaterial from Basalt Rock of Local Lampung Province.* International Journal of Technology, 13(4), 870–879.

SUPARTA, A. 2008. *Pengetahuan Bahan Glasir*. ITB Press.

WANG S, LI, X., WANG, C., BAI, M., ZHOU, X., ZHANG, X., WANG, Y. 2022. *Anorthite-based transparent glass-ceramic glaze for ceramic tiles: Preparation and crystallization mechanism.* Journal of the European Ceramic Society, 42(3), 1132–1140.

ZHANG, Q., XU, L. S., GUO, X. 2017. I*mprovement of mechanical properties, microscopic structures, and antibacterial activity by Ag/ZnO nanocomposite powder for glaze-decorated ceramic.* Journal of Advanced Ceramics, 6(3), 269–278.